EJN fens EUROPEAN JOURNAL OF NEUROSCIENCE

European Journal of Neuroscience, Vol. 36, pp. 2347–2359, 2012 doi:10.1111/j.1460-9568.2012.08138.x

BEHAVIORAL NEUROSCIENCE

Serotonin of mast cell origin contributes to hippocampal function

Katherine M. Nautiyal,[1] Christopher A. Dailey,[2] Jaquelyn L. Jahn,[3] Elizabeth Rodriquez,[1] Nguyen Hong Son,[2] Jonathan V. Sweedler[2] and Rae Silver[1,3,4]

[1]Psychology Department, Columbia University, 406 Schermerhorn Hall, 1190 Amsterdam Ave., New York, NY 10027, USA
[2]Department of Chemistry and the Beckman Institute, University of Illinois, at Urbana-Champaign, Urbana, IL, USA
[3]Psychology Department, Barnard College, New York, NY, USA
[4]Department of Pathology and Cell Biology, Columbia University Medical Center, New York, NY, USA

Keywords: hippocampus, neurogenesis, psychoneuroimmunology, serotonin, spatial learning

Abstract

In the central nervous system, serotonin, an important neurotransmitter and trophic factor, is synthesized by both mast cells and neurons. Mast cells, like other immune cells, are born in the bone marrow and migrate to many tissues. We show that they are resident in the mouse brain throughout development and adulthood. Measurements based on capillary electrophoresis with native fluorescence detection indicate that a significant contribution of serotonin to the hippocampal milieu is associated with mast cell activation. Compared with their littermates, mast cell-deficient C57BL/6 $Kit^{W\text{-}sh/W\text{-}sh}$ mice have profound deficits in hippocampus-dependent spatial learning and memory and in hippocampal neurogenesis. These deficits are associated with a reduction in cell proliferation and in immature neurons in the dentate gyrus, but not in the subventricular zone – a neurogenic niche lacking mast cells. Chronic treatment with fluoxetine, a selective serotonin reuptake inhibitor, reverses the deficit in hippocampal neurogenesis in mast cell-deficient mice. In summary, the present study demonstrates that mast cells are a source of serotonin, that mast cell-deficient C57BL/6 $Kit^{W\text{-}sh/W\text{-}sh}$ mice have disrupted hippocampus-dependent behavior and neurogenesis, and that elevating serotonin in these mice, by treatment with fluoxetine, reverses these deficits. We conclude that mast cells contribute to behavioral and physiological functions of the hippocampus and note that they play a physiological role in neuroimmune interactions, even in the absence of inflammatory responses.

Introduction

Serotonin is implicated in hippocampal function during development and adulthood, both as a neurotransmitter and as a trophic factor (Lauder & Krebs, 1978; Altman & Normile, 1988). The best known sources of hippocampal serotonin in the brain are the median raphe nuclei (Zhou & Azmitia, 1983) while resident mast cells are another less studied source (Kushnir-Sukhov *et al.*, 2007). Like other immune cells, mast cells are born in the bone marrow. They are found in the brain of rat, mouse, dove, vole and human, with interspecies differences in their precise localization and numbers (Dropp, 1976, 1979; Persinger, 1979; Goldschmidt *et al.*, 1985; Zhuang *et al.*, 1993; Kriegsfeld *et al.*, 2003). Whether serotonin of mast cell origin participates in hippocampal function in development or adulthood has not been examined.

It is known that mast cells can synthesize and store serotonin (Marathias *et al.*, 1991; Kushnir-Sukhov *et al.*, 2007; Ringvall *et al.*, 2008). The specific mediator content of mast cell granules, however, depends on the local microenvironment in which they reside (reviewed by Marshall, 2004). Serotonergic deafferentation of the hippocampus through ablation of serotonergic neurons results in a 60–80% decrease in serotonin in the hippocampus (Altman *et al.*, 1990), suggesting that as much as 20–40% of serotonin may originate from mast cells. Determination of the role of this immune cell in hippocampal physiology and function is especially interesting given evidence for other immune system effects on an array of hippocampal functions (Yirmiya & Goshen, 2011).

The hippocampus is important in the regulation of anxiety and depressive behaviors as well as in spatial learning and memory (Scoville & Milner, 1957; Gray & McNaughton, 1983; Santarelli *et al.*, 2003). Depletion of serotonin during development has profound effects on the formation of mature hippocampal synapses (Mazer *et al.*, 1997) and on neurogenesis, apoptosis and cell differentiation (Lauder, 1990; Yan *et al.*, 1997; Gaspar *et al.*, 2003). Disruption of hippocampal serotonergic signaling during development results in profound abnormalities in affective behavior and memory in adulthood (Mazer *et al.*, 1997; Gaspar *et al.*, 2003). In adulthood, increases in serotonin promote hippocampal neurogenesis (Gould, 1999), and also affect synapse formation and dendritic plasticity (Watanabe *et al.*,

Correspondence: Dr R. Silver, [1]Psychology Department, Columbia University, as above.
E-mail: qr@columbia.edu

Received 17 December 2011, revised 23 March 2012, accepted 27 March 2012

© 2012 The Authors. European Journal of Neuroscience © 2012 Federation of European Neuroscience Societies and Blackwell Publishing Ltd

1992; Mazer *et al.*, 1997). Finally, increased serotonergic signaling in adulthood has been implicated in the behavioral effects of antidepressants (Santarelli *et al.*, 2003; Sahay & Hen, 2007).

Our previous work with mast cell-deficient B6.Cg-KitW-sh/HNihr-JaeBsmJ (W^{sh}/W^{sh}) mice suggests that brain mast cells are involved in behavioral and physiological components of anxiety-like behavior (Nautiyal *et al.*, 2008). In the present studies we use these mice to explore the contribution of mast cells to the hippocampus and to its behavioral and physiological functions. Upon application of a mast cell degranulating agent, serotonin levels within hippocampi of control mice with mast cells are ~50% higher than in their mast cell-deficient W^{sh}/W^{sh} littermates. Mast cell-deficient W^{sh}/W^{sh} mice also have decreased hippocampal neurogenesis and marked deficits in spatial learning and memory. Chronic treatment with a selective serotonin reuptake inhibitor (SSRI) reverses the deficit in neurogenesis in W^{sh}/W^{sh} mice. The results indicate that mast cells and their chemical mediators may contribute to behavioral and physiological aspects of hippocampal function, even in the absence of inflammatory responses or disease states.

Materials and methods

Animals and housing

C57BL/6 wild-type (WT) and mast cell-deficient W^{sh}/W^{sh} mice (B6.Cg-KitW-sh/HNihrJaeBsmJ, C57BL/6 background) were purchased from Jackson Laboratories (Bar Harbor, ME, USA) and bred to establish colonies at Columbia University animal facilities. The W^{sh}/W^{sh} mice were crossed with WT C57BL/6 mice to generate heterozygous ($W^{sh}/+$) mice which have brain mast cells. W^{sh}/W^{sh} mice have a naturally occurring mutation in the white spotting locus (W) which causes reduced c-kit receptor expression (Duttlinger *et al.*, 1993) and results in abnormalities in pigmentation and the inability of mast cells to differentiate from their myeloid progenitors (Kitamura & Fujita, 1989; Chen *et al.*, 2005). W^{sh}/W^{sh} mice appear normal in numbers of other hematopoietic cells (Grimbaldeston *et al.*, 2005; Galli *et al.*, 2008) and in locomotor activity (Nautiyal *et al.*, 2008). All animal care and testing was approved by the Columbia University Institutional Animal Care and Use Committee.

Mast cell localization

For studies of mast cell location in the mouse brain, WT mouse pups (n = 5 per age group) were killed at postnatal day (PN) 1, 5, 9, 12, 18 or 21 or in adulthood (38 days). An additional group of WT mice were killed at ~2 months of age (n = 3) to localize mast cells in coronal sections with respect to the hippocampus. Pups aged PN1–9 were killed by decapitation. Mice of PN12 and older were deeply anesthetized with sodium pentobarbital (200 mg/kg) and perfused transcardially with saline followed by 4% paraformaldehyde.

Behavior, neurogenesis, assays

Homozygous W^{sh}/W^{sh} and heterozygous $W^{sh}/+$ male mice (at 12–18 weeks) from $W^{sh}/W^{sh} \times W^{sh}/+$ crosses were used in serotonin, behavior, neurogenesis and corticosterone experiments. Animals for neurogenesis experiments were anesthetized with sodium pentobarbital and killed by transcardial perfusion as described above. Animals used in brain serotonin and plasma corticosterone assays were killed by decapitation. Trunk blood was collected and brains were rapidly removed from crania and placed in ice-cold Hank's balanced salt solution (HBSS; Invitrogen, Carlsbad, CA, USA).

Housing

Following weaning at 28 days, mice were housed 2–5 per cage in transparent plastic bins (36 × 20 × 20 cm) under a 12/12-h light-dark cycle at 22 ± 1 °C. Cages had corn cob bedding (Bed-o'cobs, Maumee, OH, USA) and food and water were provided *ad libitum*.

Treatments

BrdU injections

5-Bromo-2′-deoxyuridine (BrdU; Sigma Aldrich, St. Louis, MO, USA) was used to label dividing cells. For assessment of cell proliferation and survival in the dentate gyrus (DG), $W^{sh}/+$ and W^{sh}/W^{sh} mice were injected once daily for 3 days with BrdU at a dose of 150 mg/kg i.p. (concentration 7.5 mg/mL saline) and killed 24 h following the third injection. For assessment of cell survival in the DG and olfactory bulb, mice were killed 28 days following the third injection. For assessment of cell proliferation in the subventricular zone (SVZ) and following SSRI administration, mice were injected once with BrdU (150 mg/kg, i.p.) and killed 24 h later.

SSRI administration

$W^{sh}/+$ and W^{sh}/W^{sh} mice were given once-daily i.p. injections of fluoxetine hydrochloride at a dose of 10 mg/kg/day (concentration of 1 mg/mL saline; Biotrend AG, Zurich, Switzerland) or saline vehicle. Following 28 days of treatment, mice were tested in the open field and novelty suppressed feeding tests. One week later mice were injected with BrdU.

Assays

Measurements of serotonin via capillary electrophoresis-laser induced native fluorescence

As seen in Fig. 1, mast cells lie within and near the hippocampus. Upon activation, mast cell granules release their contents over a substantial volume of tissue (Ruoss *et al.*, 1991; Marszalek *et al.*, 1997; Nautiyal *et al.*, 2008). Thus, following degranulation, granular contents from mast cells lying both within and near the hippocampus can be measured. To measure the contribution of mast cells to the hippocampal milieu, coronal slices were cut on a vibratome (300 μm) in ice-cold HBSS. The caudal hippocampal slice (bregma −2.92 mm) was chosen as this is a region rich in mast cells. The rostral hippocampal slice (bregma −1.70 mm) served as a control as this region bears few mast cells.

To measure the contribution of mediators of mast cell origin, degranulation was induced by applying 400 μL of Compound 48/80 (C48/80; Sigma Aldrich) at a concentration of 0.1 mg/mL in HBSS, while the mast cells, contribution at baseline was examined after application of HBSS alone. The brain slice was incubated with C48/80 or the HBSS vehicle for 3 min. Next, the hippocampus was dissected out and placed into Eppendorf tubes, weighed and manually homogenized in 20 μL of extraction matrix [49.5% LC-MS Chromasolve Methanol (Sigma Aldrich), 49.5% LC/MS grade water (Thermo Scientific, Waltham, MA, USA), 1% acetic acid (Sigma Aldrich)] per mg of dissected tissue. Homogenized tissue was incubated with extraction matrix for 90 min at 4 °C before centrifugation at 15 000 ***g*** for 15 min. The supernatants were then transferred to PCR tubes and frozen at −80 °C until analysis by capillary electrophoresis with laser induced native fluorescence (CE-LINF).

Each sample was analysed in triplicate using a laboratory-built CE-LINF instrument equipped with a wavelength-resolved detector

© 2012 The Authors. European Journal of Neuroscience © 2012 Federation of European Neuroscience Societies and Blackwell Publishing Ltd

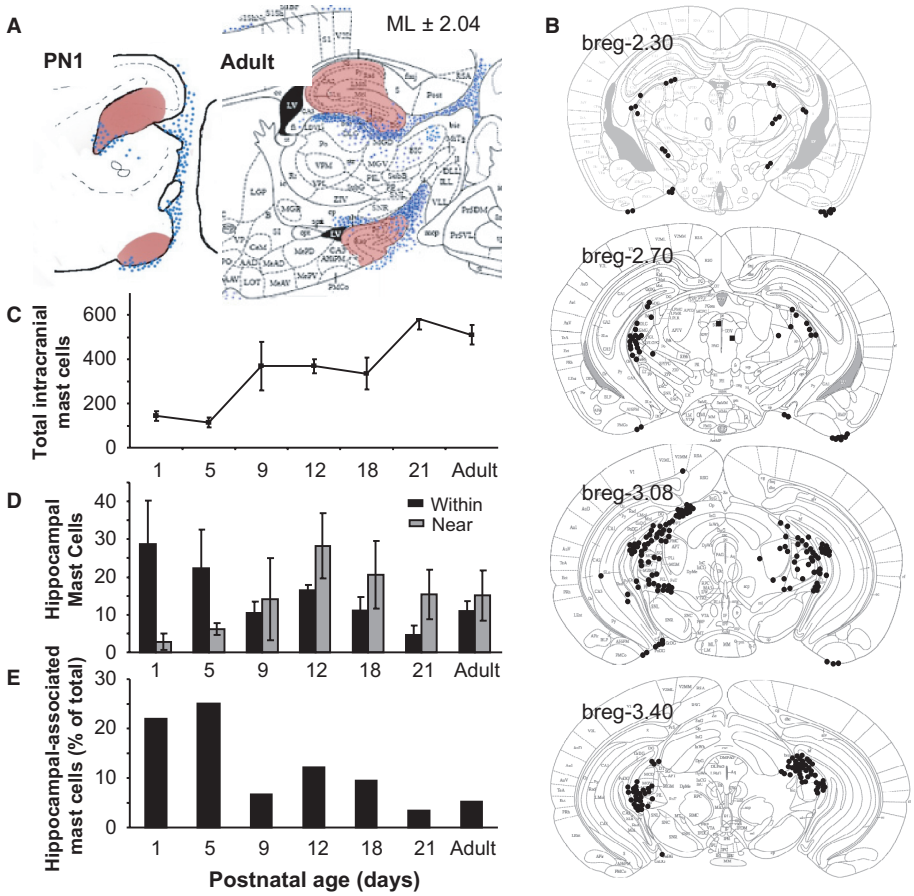

FIG. 1. Mast cell location in the brain. (A) Sagittal view of the location of mast cells in PN1 and adult mice. Each dot represents one mast cell (blue) in relation to the hippocampus (red). Mast cells are located in the parenchyma of the hippocampus as well as the leptomeninges adjacent to the hippocampus. (B) Coronal view of adult brain depicting the intracranial location of mast cells from bregma −2.30 to −3.40 mm with each dot representing one mast cell. (C) The total number of intracranial mast cells (mean ± SEM) and (D) the number of mast cells within or near the hippocampal formation is shown throughout development. (E) Percentage of the total population that these mast cells comprise (within and near hippocampus/total brain mast cells × 100).

similar to that previously described (Fuller *et al.*, 1998; Squires *et al.*, 2007). Briefly, 10 nL of the supernatant was hydrodynamically injected into a fused silica capillary and 21 kV applied for separation. Eluting analytes were excited via 264-nm radiation from a frequency-doubled argon ion laser. The native fluorescence was collected and the spectrum imaged onto a CCD array where it was recorded at a rate of 2 Hz. The peaks resulting from the elution of serotonin were identified by comparison of both migration time and fluorescence characteristics to a standard of serotonin (Sigma Aldrich) spiked into extraction matrix. For quantification, the total integrated signal was calculated from the electropherograms by comparison to a linear working curve derived from five serotonin standards of known concentration (15–250 nM) and was then normalized to the weight of dissected hippocampal tissue. Outlying data points were removed based on the results of the Q-test. If either of the two sections of hippocampus was found to be a statistical outlier the corresponding data for the remaining section of hippocampus was removed. Differences in the populations were evaluated by Kruskal–Wallis non-parametric analysis using ORIGIN 8.0 (Kruskal & Wallis, 1952). We also measured tyrosine (Tyr), and tested for the presence of several serotonin-related catabolites [HIAA (5-hydroxyindoleacetic acid), serotonin sulfate, HITCA (5-hydroxyindole thiazoladine carboxylic acid), NAS (*N*-acetylserotonin): see Squires *et al.* (2007)]. These catabolites were below the instrument's limit of detection and are therefore not reported here.

Plasma corticosterone

Mice were killed by decapitation within 2 h following lights on and trunk blood was collected into EDTA-coated tubes (BD, Franklin Lakes, NJ, USA) and spun down at 4 °C at 1400 ***g*** for 15 min. Plasma was collected and stored at −80 °C until processed. Plasma corticosterone was assayed using a commercially available EIA kit (Cayman Chemical, Ann Arbor, MI, USA) according to the manufacturer's directions. Samples were run in duplicate at two dilutions with resulting concentrations falling on the linear portion of the standard curve. The coefficient of variation between duplicates was less than 7%; otherwise the samples were rerun.

Tissue processing

For mast cell localization during development, the crania were cleaned of skin, muscles and lower jaw structure and post-fixed in 4% paraformaldehyde overnight. Post-fixed crania were placed in a mild formic acid bone decalcifier (Immunocal, Tallman, NY, USA) for 24 h, then washed in water and phosphate buffer (pH 7.3) and then embedded in gelatin. Brains were cut into 50-μm-thick sagittal (for developmental study) or coronal (for adult hippocampal localization) sections on a cryostat (Microm HM 500M, Walldorf). Sections were thaw-mounted onto slides (Probe-on-plus slides; FisherBrand, Waltham, MA, USA), and stored at −80 °C until processed.

© 2012 The Authors. European Journal of Neuroscience © 2012 Federation of European Neuroscience Societies and Blackwell Publishing Ltd

Mast cell staining

Slide-mounted sections were stained with the acidic (pH 2.0) toluidine blue (TB) stain (Sigma), a commonly used marker for mast cells reported both in our work (e.g. Silverman *et al.*, 1994; Zhuang *et al.*, 1999; Wilhelm *et al.*, 2000) and by many other labs (e.g. Florenzano *et al.*, 2000; Esposito *et al.*, 2001; Menétrey *et al.*, 2003). Acidic toluidine has metachromatic properties and color changes to a deep blue/purple in tissues with acidic polyanions such as the proteogylcans and heparin found in mast cell granules (Presnell & Schreibman, 1997). Confirmation of the mast cell identity of TB-stained cells has previously been confirmed in the brain by double labeling with alcian and/or safrinin and based on ultrastructural evidence using electron microscopy (Silverman *et al.*, 1994; Yang *et al.*, 1999; Zhuang *et al.*, 1999). In the present study, for TB staining, slides were washed in 60% EtOH for 2 min, stained with TB (4 mg/mL TB in 60% EtOH, pH 2.0), washed briefly in distilled water, dehydrated through a series of ethanols (50% for 15 s, 70% for 45 s, 2 × 95% for 1 min, 2 × 100% for 1 min), cleared in Citrasolv (3 × 5 min) and coverslipped with Permount.

To confirm the identity of the mast cells, additional slide-mounted sections were initially stained with avidin, which labels mast cells by binding to the heparin found in mast cells (Bussolati & Gugliotta, 1983; Tharp *et al.*, 1985; Presnell & Schreibman, 1997). Next, the sections were photographed, the coverslip was removed and the sections were re-stained with TB (as described above) to show double-labeling of brain mast cells with avidin and TB. For avidin staining, slides were washed in phosphate buffer (PB) with 0.1% triton X (PBT), then incubated in PBT with Cy3-conjugated egg-white avidin (1 : 5000; Jackson ImmunoResearch, West Grove, PA, USA) for 2 h. Slides were then washed in PB, dehydrated, cleared in n-xylenes and coverslipped with Krystalon.

Analysis of mast cell localization

Every fourth section through the brain was analysed by two observers for the number and location of mast cells using a light microscope (BH-2; Olympus America Inc., Center Valley, PA, USA; inter-rater reliability: $r^2 > 0.95$). Mast cells were identified by their deep purple granules against the light blue background Nissl stain. The location of each mast cell was mapped using a brain atlas (Paxinos & Franklin, 2004). Mast cells were localized to the following regions: olfactory bulb, cortex, hippocampus, amygdala, thalamus, hypothalamus and cerebellum, and included mast cells located within the parenchyma as well as those in the perivascular spaces, choroid plexus and meningeal layers.

Immunohistochemistry for neurogenesis

Perfused brains of animals injected with BrdU were post-fixed overnight, submerged in sucrose for 48 h, then cut into 50-μm coronal sections on a cryostat (Microm HM 500M, Walldorf) and placed in PB. Every eighth section of hippocampus and olfactory bulb and every fourth section of the SVZ was processed by free-floating immunohistochemistry as previously described (Meshi *et al.*, 2006). In brief, sections were washed in Tris-buffered saline (TBS), denatured in 50% formamide/2 × saline sodium citrate (SSC) at 60 °C, washed in SSC, then in HCl at 37 °C and boric acid, then again in TBS. Sections were incubated for 36 h at 4 °C in primary antibodies against one or two of the following antigens: BrdU (AbD Serotec Cat# OBT0030G, Raleigh, NC, USA; 1:200), doublecortin (DCX; Santa Cruz Biotechnology Cat# sc-8066, Santa Cruz, CA, USA; 1 : 1000), neuronal-specific nucleus protein (NeuN) (Chemicon Cat# MAB377, Billerica, ME, USA; 1:500). Sections were then washed and incubated in the appropriate fluorescent secondary antibodies – donkey anti-rat secondary conjugated to CY3 for BrdU, donkey anti-goat conjugated to CY2 for DCX, and donkey anti-mouse conjugated to CY2 for NeuN (Jackson ImmunoResearch, 1 : 200) for 2 h, then washed, mounted, dehydrated and coverslipped.

Immunohistochemistry for c-kit receptor

Perfused mouse brains were post-fixed overnight, then submerged in sucrose for 48 h, then cut into 50-μm coronal sections on a cryostat (Microm HM 500M, Walldorf) into PB. Every eighth free-floating section of hippocampus and cerebellum was processed for double-labeled immunohistochemistry against c-kit and either glial fibrillary acidic protein (GFAP) or DCX. In brief, sections were washed in PB with PBT, blocked in normal donkey serum, then incubated overnight in rabbit anti-c-kit receptor primary antibody (Ab-1; Oncogene Research Products, Cat# PC-34, Boston, MA, USA; 1:500) and either goat anti-GFAP (C-19, Santa Cruz Biotechnology, Cat# sc-6170, 1 : 250) or goat anti-DCX (as above). Sections were then washed and incubated in PBT with fluorescent secondary antibodies – donkey anti-rabbit secondary conjugated to CY3 for c-kit, donkey anti-goat conjugated to CY2 for GFAP and DCX for 2 h. Slides were then washed in PB and coverslipped with ProLong Gold (Invitrogen, Grand Island, NY, USA).

Analysis of immunostained sections

Images of single labeled sections were captured using a Nikon Eclipse E800 light microscope (Nikon Co., Tokyo, Japan) equipped with the green fluorescent protein (GFP) (480 ± 20 nm) or Texas Red (560 ± 40 nm) filters to detect CY2 or CY3 fluorophores, respectively. The microscope is fitted with a Q-Imaging Retiga EXi, fast 1394 camera (Quantitative Imaging, Surrey, BC, Canada) with QCapture software (version 2.95.0; Quantitative Imaging). Images were loaded into Photoshop 7.0 (Adobe Systems, San Jose, CA, USA) for cell counting.

BrdU+ cells were counted by two observers blind to genotype and condition (inter-rater reliability: $r^2 > 0.95$). Sampling of BrdU+ cells was performed as follows: six sections per animal in DG along the subgranular layer; four sections per animal in SVZ adjacent to the lateral ventricle olfactory bulb; four sections per animal, scored in three representative areas (0.1 × 0.1 mm), randomly placed in the granule cell layer (GCL) of the olfactory bulb. Area of staining, rather than cell counting, was used to quantify the DCX staining in six sections of the hippocampus in every animal in ImageJ 1.31 with the Otsu method to determine the threshold of positive staining (Otsu, 1979).

Double labeling of cells with BrdU and NeuN in the GCL was assessed by first counting the number of BrdU cells as described above in Photoshop (Adobe). Numbers of cells labeled with both BrdU and NeuN were then counted amongst the population of BrdU+ cells. Confocal microscopy was used to confirm double labeled BrdU and NeuN cells. Specifically, the bilateral hippocampus from one representative section (bregma −2.2) per animal was scanned with a Zeiss Axiovert 200 MOT fluorescence microscope (Carl Zeiss, Thornwood, NY, USA) with Zeiss LSM 510 laser scanning confocal attachment and LSM 3.95 software (Carl Zeiss). Cells within the captured images were examined in 2-μm optical slices using the LSM 3.95 software for confirmation of double labeling. The percentage of double labeled cells achieved with both methods was not different ($r^2 > 0.95$, $P < 0.01$).

The volume of the DG was estimated using the Cavalieri method (Gundersen & Jensen, 1987). Briefly, the area of the NeuN+ DG was

© 2012 The Authors. European Journal of Neuroscience © 2012 Federation of European Neuroscience Societies and Blackwell Publishing Ltd

measured in six sections of the hippocampus in each animal in ImageJ 1.31 with the Otsu method to determine the threshold of positive staining. The volume of the hippocampus was calculated by multiplying the area of the hippocampal staining in each section obtained from ImageJ (in μm^2) by the thickness of the section plus the distance between sections (50 + 150 μm). The total volume was calculated by summing this volume across the six sections.

Behavioral tests

Radial arm maze

For assessment of spatial learning and memory, $W^{sh}/+$ and W^{sh}/W^{sh} mice were tested in the radial arm maze. Animals were weighed once per day and kept on a restricted feeding paradigm to maintain their body weight at 80–85% of their free-feeding weight. The radial arm maze was made of black plexiglass with eight arms extending 50 cm from the center, with 16-cm-high walls. Racks and other behavioral testing equipment in the room served as spatial cues. Mice were tested twice daily in the maze (2 and 8 h after lights on). Mice were placed in the center of the radial arm maze restricted to a plexiglass cylinder for 15 s. The cylinder was then lifted and the session began, lasting 10 min or until all rewards were retrieved and eaten. Each session was videotaped and the maze was wiped down with 70% ethanol following each animal. Mice were given three habituation sessions during which pieces of Fruit Loops® (Kellogg's) were scattered throughout the maze and then placed at the end of each arm. Mice were given 20 training trials in which three arms were baited with Fruit Loops pieces, followed by a reversal trial in which three different arms were baited. Each arm entered, latency to enter the first arm and latency to retrieve bait were measured. An entry into an arm was scored as an error if the mouse had already entered that arm during the trial (working memory error), or if the arm did not contain a reward (reference memory error). Other behaviors recorded include grooming, rearing, investigation of potential food location (weigh-boat) and scratching/biting weigh-boat. None of these behaviors was significantly different between genotypes and are therefore not reported here.

Morris water maze

For further assessment of hippocampus-dependent spatial learning, mice were tested in the Morris water maze (Morris, 1984). A 150-cm-diameter round pool was filled with water (25 °C, 10 cm deep) and made opaque by the addition of non-toxic white tempera paint. Four black and white patterns (small checked, large vertical stripes, small horizontal stripes, large circle) on 8½ × 11-inch paper were placed on the inside wall of the Morris water maze to serve as spatial cues. Mice were subject to four trials daily, for 9 days. Mice were videotaped during each trial (Sony Handycam) and CleverSys software was used for analysis of swim path and time spent in each quadrant.

Mice were placed in the pool at each of four drop points (N, E, S, W) randomized between days, but kept consistent for all animals within a given day. Basic black and white patterned cues were placed at each of the four drop points above the water line to serve as spatial cues. A plexiglass platform (10 × 10 cm) was weighted down and placed in the center of the SE quadrant. Time to reach the platform was recorded for each trial (escape latency) in seconds. Mice were allowed 90 s to reach the platform, on which they had to remain for 5 s before being removed by the experimenter. If a mouse did not reach the platform within the 90 s, a latency of 90 s was assigned and the mouse was gently guided by the experimenter to the platform before being removed from the water. A visible platform was used on the first day for shaping trials. It was elevated 1 cm from the water surface and clearly marked with a flag. For hidden platform trials, the platform was 1 cm below the water. On the sixth day, a single probe trial was run; the platform was removed from the pool and the swim path and time spent in the target quadrant was analysed. On days 7–9, visible platform trials were run to assess non-spatial deficits such as swimming performance or sensory perception. Mice were always placed in the pool at the E drop point, and the location of the platform placement was varied among the centers of each of the quadrants.

Statistics

Two-tailed Student's *t*-tests were used to compare hippocampal volume measurements, BrdU+ cell counts, DCX staining area and plasma corticosterone levels between genotypes. If the test for normality failed, a Mann–Whitney Rank Sum Test was run. A chi-square test was used to test differences in cell survival between genotypes. Two-way ANOVAs were used to assess effects of genotype and trial in behavioral experiments, and also effects of genotype and treatment in the SSRI experiment. Tukey's HSD was used for *post-hoc* testing when appropriate.

Results

Mast cell location in development

The number and localization of intracranial mast cells was studied throughout development and in adulthood (Fig. 1). In mice, mast cells are located in the meninges and perivascular spaces on the brain side of the blood–brain barrier predominantly in thalamic and hippocampal brain regions (Hendrix *et al.*, 2006; Kovács & Larson, 2006; Nautiyal *et al.*, 2011). Brain maps, seen in sagittal (Fig. 1A) and coronal (Fig. 1B) views revealed mast cells around the hippocampus, where they lie predominantly in more caudal areas (bregma −3.08). The total number of intracranial mast cells increased steadily after birth, reaching adult levels around PN21 ($F_{6,30} = 7.4$, $P < 0.01$; Fig. 1C). The total number of mast cells located within the parenchyma of the hippocampus and surrounding leptomeninges remained stable over this interval, with a gradual shift from the former to the latter compartment (Fig. 1D). Thus, a larger proportion of total brain mast cells are located in and around the hippocampus during early postnatal development, peaking at around 25% at PN5 (Fig. 1E).

Mast cells, stained with both TB and avidin, are seen within the brain (Fig. 2A). Mast cells are located in the parenchyma of the hippocampus as well as the leptomeninges and choroid plexus adjacent to the hippocampus (Fig. 2B). These results, together with previous work showing altered anxiety-like behavior in mast cell-deficient mice (Nautiyal *et al.*, 2008), led us to focus on mast cell functions in the hippocampus.

Hippocampal serotonin of mast cell origin

To investigate mast cell contribution of serotonin to the hippocampus, C48/80 (a mast cell degranulating agent) or control HBSS solution was applied to brain slices containing the caudal or the rostral hippocampus. The total serotonin content was subsequently measured in the dissected hippocampal parenchyma at two rostral–caudal levels using CE-LINF detection. Our laboratory-built instrument allows for the trace analysis of natively fluorescent analytes from volume-limited samples, including indoles in the hippocampus (Fuller *et al.*, 1998; Hatcher *et al.*, 2008). Analysis of both rostral and caudal regions of the hippocampus in mast cell-deficient W^{sh}/W^{sh} and mast cell-competent $W^{sh}/+$ mice revealed that mast cells contribute significantly

© 2012 The Authors. European Journal of Neuroscience © 2012 Federation of European Neuroscience Societies and Blackwell Publishing Ltd

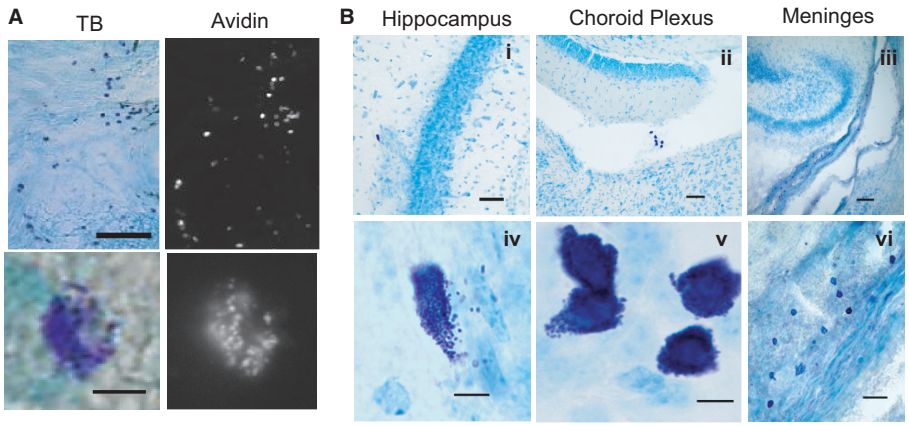

FIG. 2. Mast cells in the brain at low (upper panels) and high (lower panels) magnification. (A) Mast cells are stained with toluidine blue (left) and avidin (right). (B) Photomicrographs of toluidine blue-stained mast cells located within the hippocampal parenchyma (i, iv) or meninges (ii, iii, v, vi) near the hippocampus. Scale bars = 100 μm (upper panels); 5 μm for A (bottom panels) and B iv, v; and 60 μm for B vi.

to the serotonin content in the caudal but not rostral hippocampus in $W^{sh}/+$ mice (Fig. 3).

In the rostral hippocampus, there were no significant differences between $W^{sh}/+$ ($n = 4$) and W^{sh}/W^{sh} ($n = 5$) mice in baseline levels of serotonin, measured following application of HBSS vehicle ($H_1 = 0.00$, $P > 0.05$; Fig. 3A). Additionally, following application of C48/80, there were no differences in serotonin content in the rostral hippocampus between $W^{sh}/+$ ($n = 7$) and W^{sh}/W^{sh} ($n = 7$) mice ($H_1 = 0.10$, $P > 0.05$; Fig. 3B).

In the caudal hippocampus, there were no significant differences between $W^{sh}/+$ and W^{sh}/W^{sh} mice in baseline levels of serotonin measured in the HBSS vehicle condition ($H_1 = 0.02$, $P > 0.05$; Fig. 3A). In contrast, following application of C48/80 to slices, serotonin content in $W^{sh}/+$ mice ($n = 7$) was increased compared with their HBSS baseline and with that of W^{sh}/W^{sh} ($n = 8$) mice ($H_1 = 6.48$, $P < 0.05$). Approximately 50% more serotonin was measured in $W^{sh}/+$ mice compared with W^{sh}/W^{sh} mice in the C48/80-stimulated caudal hippocampus. This represents a dynamic mast cell-mediated increase in serotonin in the hippocampus. Interestingly this increase corresponds to the larger population of mast cells resident near the caudal vs. rostral hippocampus in adulthood and indicates that degranulation of mast cells in brain tissue contributes measurable levels of this neurotransmitter to the hippocampal milieu.

In measuring serotonin with our CE-LINF instrument, Tyr (not found in mast cells) was also measured. As expected, levels in $W^{sh}/+$ and W^{sh}/W^{sh} animals did not change with mast cell stimulation by C48/80 (data not shown).

Spatial learning and memory

Radial arm maze

W^{sh}/W^{sh} mice showed deficits in hippocampus-dependent spatial learning and memory in the radial arm maze (Fig. 4A). Both W^{sh}/W^{sh} ($n = 4$) and $W^{sh}/+$ ($n = 5$) littermates reduced the number of errors made over the five training blocks, suggesting that they learned to locate the rewards ($F_{5,35} = 12.42$, $P < 0.05$). There were no significant differences between $W^{sh}/+$ and W^{sh}/W^{sh} mice in the number of errors made during training trials ($F_{1,35} = 0.06$, $P > 0.05$) nor in the total number of errors made in the last training block (4.2 ± 0.5 and 3.9 ± 0.5, respectively; $t_7 = 0.71$, $P > 0.05$). However, on the reversal trial, the total number of errors increased from the last training block in

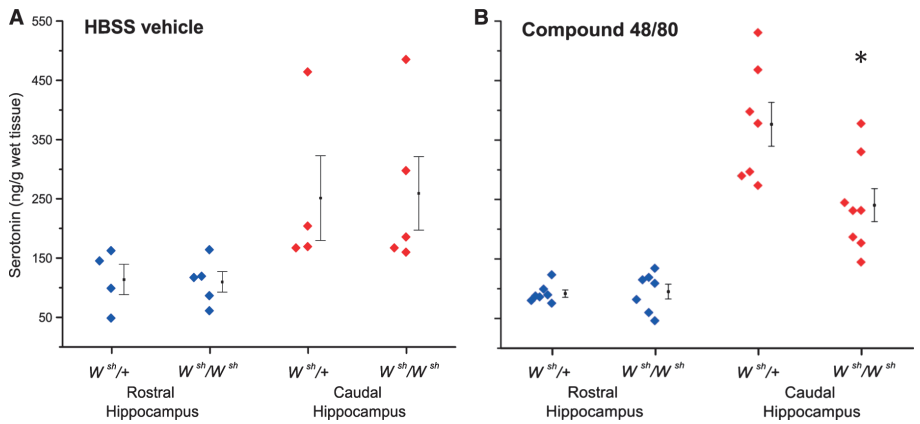

FIG. 3. Effects of mast cell degranulation on hippocampal serotonin content in mast cell-deficient W^{sh}/W^{sh} and $W^{sh}/+$ mice. The contribution of mast cells to serotonin content in the rostral (blue) and caudal (red) hippocampus is shown following stimulation with (A) HBSS vehicle or (B) C48/80. There were no significant differences between genotypes in either rostral or caudal hippocampus following HBSS vehicle application or in rostral hippocampal slices stimulated with C48/80. However, in brain slices from $W^{sh}/+$ but not W^{sh}/W^{sh} mice, there were increases in serotonin in the caudal hippocampus following stimulation with C48/80. *$P < 0.05$.

© 2012 The Authors. European Journal of Neuroscience © 2012 Federation of European Neuroscience Societies and Blackwell Publishing Ltd

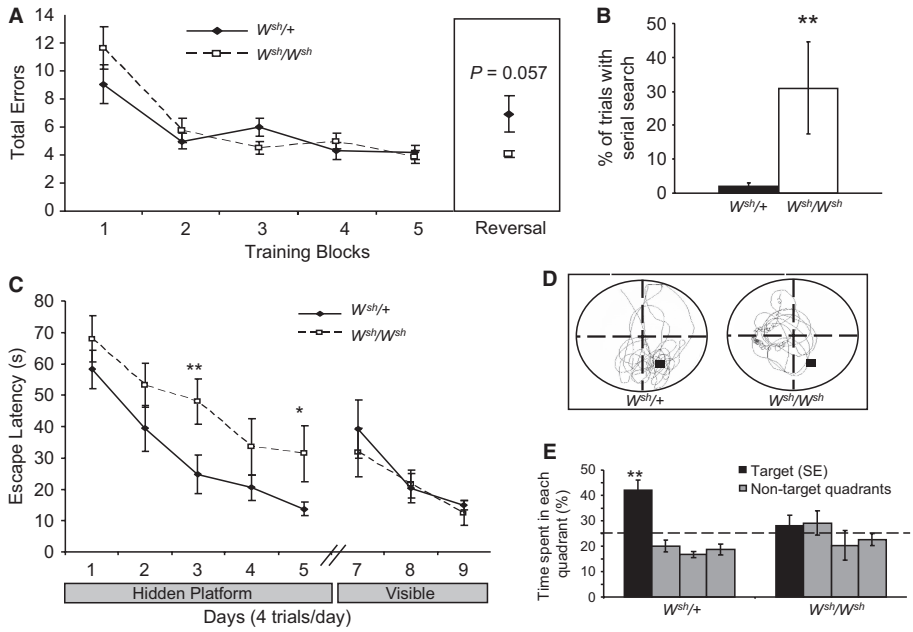

FIG. 4. Spatial memory in $W^{sh}/+$ and W^{sh}/W^{sh} mice in radial arm and Morris water mazes. (A) The number of errors in the radial arm maze for training and reversal trials. (B) The percentage of trials in which mice performed a serial search. (C) Escape latency in the Morris water maze over hidden and visible platform trials. (D) Representative swim paths of $W^{sh}/+$ and W^{sh}/W^{sh} mice during the probe trial. Dashed lines demarcate quadrants and the gray box indicates the location of the platform during training. (E) Percentage of time spent in each target and non-target quadrant of the pool during the probe trial for $W^{sh}/+$ and W^{sh}/W^{sh} mice. Dashed line indicates chance performance (25%). *$P < 0.05$, **$P < 0.01$.

Wsh/+ mice ($t_8 = 2.21$, $P = 0.057$), with the W^{sh}/W^{sh} mice making fewer total errors than their littermates during the reversal trial (4.3 ± 0.3 vs. 7.2 ± 1.3: $F_{1,14} = 4.31$, $P = 0.057$). Interestingly, in W^{sh}/W^{sh} mice, there was no increase in the number of reference memory errors (entries into unbaited arms) in the reversal trial, indicating that they did not learn the location of the rewards based on spatial cues. Rather, their seemingly successful performance is due to a learned non-spatial search strategy, in which working memory errors (re-entries into arms) are low (Hodges, 1996). In keeping with this idea, analysis of the pattern of arm entries in W^{sh}/W^{sh} mice revealed a serial search pattern (Fig. 4B). Serial search is defined as entering successive arms in a clockwise or counterclockwise fashion during a single trial. Over 21 trials (training + reversal), W^{sh}/W^{sh} mice performed an exact match serial search 30.9% of the time while control mice did so only 1.9% of the time ($t_7 = 2.43$, $P < 0.05$) supporting the suggestion that W^{sh}/W^{sh} mice were not learning the location of the rewards.

Morris water maze

W^{sh}/W^{sh} mice also showed impaired learning and memory in the Morris water maze test of hippocampus-dependent spatial learning (Fig. 4C). Compared with $W^{sh}/+$ mice ($n = 9$), W^{sh}/W^{sh} mice ($n = 8$) took longer to reach the hidden platform (Fig. 4C; $F_{1,59} = 5.61$, $P < 0.05$). By the fifth day, $W^{sh}/+$ mice reached the platform in 13 ± 5 s while W^{sh}/W^{sh} mice took 31 ± 6 s ($t_{15} = 2.04$, $P = 0.059$). Collapsed across both genotypes, the escape latency decreased over days (main effect of time; $F_{4,59} = 17.05$, $P < 0.01$). There was no significant difference between genotypes in escape latency in the visible platform trials, indicating competence in motor and sensory systems in W^{sh}/W^{sh} mice. Performance during the probe trial indicates impairments in spatial learning and memory in W^{sh}/W^{sh} mice. There was a difference between genotypes in the amount of time spent in each quadrant ($W^{sh}/+$ vs. W^{sh}/W^{sh}: $t_{15} = 2.45$, $P < 0.05$; Fig. 4D).

TABLE 1. Volume (mm^3) of the dentate gyrus and CA1–CA3 regions of the hippocampus for $W^{sh}/+$ and littermate W^{sh}/W^{sh} mice

Volume (mm^3) Genotype	Dentate gyrus (X ± SEM)	CA1–CA3 (X ± SEM)
$W^{sh}/+$	0.221 ± 0.007	0.498 ± 0.017
W^{sh}/W^{sh}	0.192 ± 0.005*	0.48 ± 0.027

*$P < 0.01$ for $W^{sh}/+$ vs. W^{sh}/W^{sh} mice in dentate gyrus.

$W^{sh}/+$ mice spent significantly more of their time in the target quadrant compared with the other three (42%; $F_{3,32} = 20.81$, $P < 0.01$). In contrast, W^{sh}/W^{sh} mice spent only 28% of their time in the target quadrant, the same as the amount of time spent in any other quadrant ($F_{3,28} = 0.94$, $P > 0.05$; Fig. 4E), indicating a lack of learning and/or memory of the location of the platform.

Neurogenesis

Hippocampal volume

The volume of the GCL of the DG in W^{sh}/W^{sh} mice ($n = 8$) was reduced by 12.9% compared with littermate $W^{sh}/+$ controls ($n = 10$; $t_{16} = 3.22$, $P < 0.01$). There was no difference in the volume of CA1–CA3 regions ($t_{16} = 0.94$, $P > 0.05$; Table 1).

Cell proliferation

Cell proliferation was assessed by incorporation of BrdU into dividing cells (Fig. 5A). There was a 43.5% reduction in the number of proliferating cells in the GCL of the DG in W^{sh}/W^{sh} mice ($n = 9$) compared with $W^{sh}/+$ littermates ($n = 12$) over several rostral-caudal levels (75.2 ± 15.0 vs. 133.1 ± 14.7; $t_{19} = 2.73$, $P < 0.05$; Fig. 5B and C). There were no significant effects of genotype on cell proliferation in another neurogenic niche, the SVZ, where no mast

© 2012 The Authors. European Journal of Neuroscience © 2012 Federation of European Neuroscience Societies and Blackwell Publishing Ltd

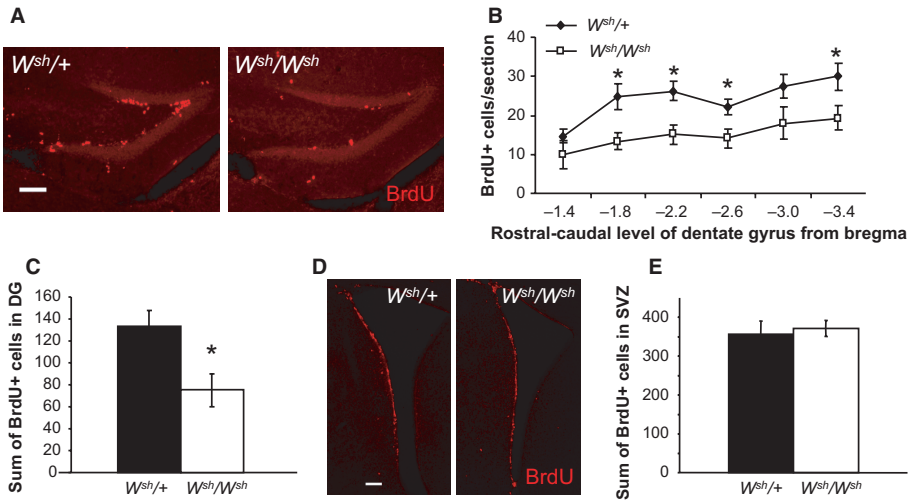

FIG. 5. Cell proliferation in dentate gyrus and subventricular zone in $W^{sh}/+$ and W^{sh}/W^{sh} mice. (A) Representative photomicrographs showing BrdU staining in the dentate gyrus (bregma −1.8 mm). (B) The number of BrdU+ cells across the rostral–caudal extent of the dentate gyrus. (C) Histogram of BrdU+ cells in the dentate gyrus. (D) Representative photomicrographs of BrdU staining in the SVZ. (E) Histogram of the number of BrdU+ cells in the SVZ . $^*P < 0.05$. Scale bars = 100 μm.

cells are found. $W^{sh}/+$ mice had 356.1 ± 34.0 while W^{sh}/W^{sh} mice had 371.8 ± 20.6 BrdU+ cells in the SVZ (Fig. 5D and E; $t_9 = 0.49$, $P > 0.05$).

Doublecortin staining

We stained for DCX, a marker of immature neurons, to determine if the reduction in cell proliferation applied to cells of neuronal fate (Fig. 6A). W^{sh}/W^{sh} mice ($n = 8$) had reduced DCX immunoreactivity compared with $W^{sh}/+$ controls ($n = 8$), with a total area of staining of 0.08 ± 0.01 mm^2 in W^{sh}/W^{sh} mice compared with 0.11 ± 0.01 mm^2 in $W^{sh}/+$ controls (Fig. 6B; $t_{14} = 3.06$, $P < 0.01$).

Cell survival and phenotype

There was a 26.8% reduction in the number of BrdU+ cells in the GCL of the DG in W^{sh}/W^{sh} mice ($n = 9$) compared with $W^{sh}/+$ controls ($n = 8$) 28 days after BrdU injection ($t_{15} = 2.38$, $P < 0.05$). Given the reduction in cell proliferation in W^{sh}/W^{sh} mice, there was no significant difference in cell survival between genotypes ($\chi^2 = 0.53$, $P > 0.05$; Fig. 7A).

BrdU and NeuN co-localization in animals used in the cell survival study was examined to determine if differentiation of new cells in the dentate gyrus was affected in W^{sh}/W^{sh} mice (Fig. 7B). In W^{sh}/W^{sh} mice ($n = 9$), 63.4 ± 2.8% of BrdU-labeled cells were NeuN positive, compared with 51.9 ± 4.6% in $W^{sh}/+$ mice ($n = 8$; $t_{15} = 1.76$, $P = 0.11$). Although this difference was not statistically significant, this suggestive increase in BrdU+NeuN+ cells in W^{sh}/W^{sh} mice may represent a compensatory increase in neuron fate due to the reduced cell proliferation.

There were no significant effects of genotype on cell survival in the olfactory bulb (Fig. 7C and D). $W^{sh}/+$ ($n = 9$) and W^{sh}/W^{sh} ($n = 8$) mice had similar numbers of BrdU+ cells per 100 μm^3 of tissue within the GCL of the olfactory bulb, 34.67 ± 1.53 and 34.29 ± 0.98, respectively ($t_{15} = 0.2$, $P > 0.05$).

Plasma corticosterone assay

Given the known effects of chronically elevated corticosterone on hippocampal neurogenesis (Gould *et al.*, 1991) and the anxiety phenotype of W^{sh}/W^{sh} mice (Nautiyal *et al.*, 2008), we measured plasma corticosterone to assess whether the reduction in cell proliferation in W^{sh}/W^{sh} mice was associated with stress. There were no significant differences in baseline levels of plasma corticosterone

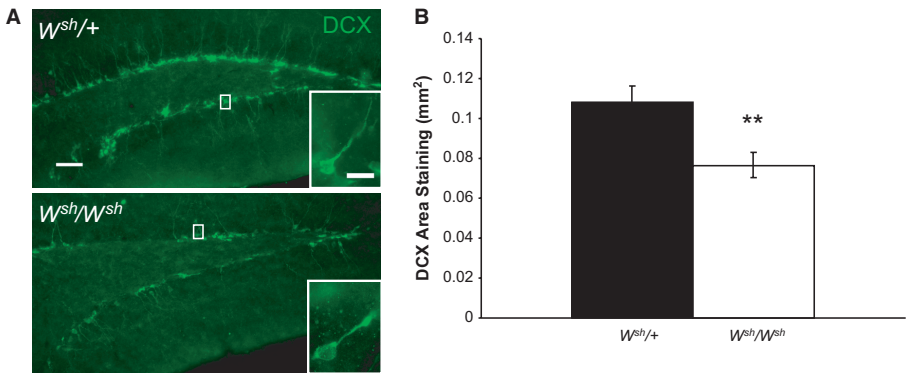

FIG. 6. Immature neurons in the dentate gyrus in $W^{sh}/+$ and W^{sh}/W^{sh} mice. (A) Representative photomicrographs of DCX staining in the dentate gyrus of $W^{sh}/+$ and W^{sh}/W^{sh} mice. The small white box shows the location of the high-magnification inset. Scale bar = 100 μm for hippocampal photomicrograph, 12 μm for inset. (B) Histogram of the area of DCX staining in the dentate gyrus. $^{**}P < 0.01$.

© 2012 The Authors. European Journal of Neuroscience © 2012 Federation of European Neuroscience Societies and Blackwell Publishing Ltd

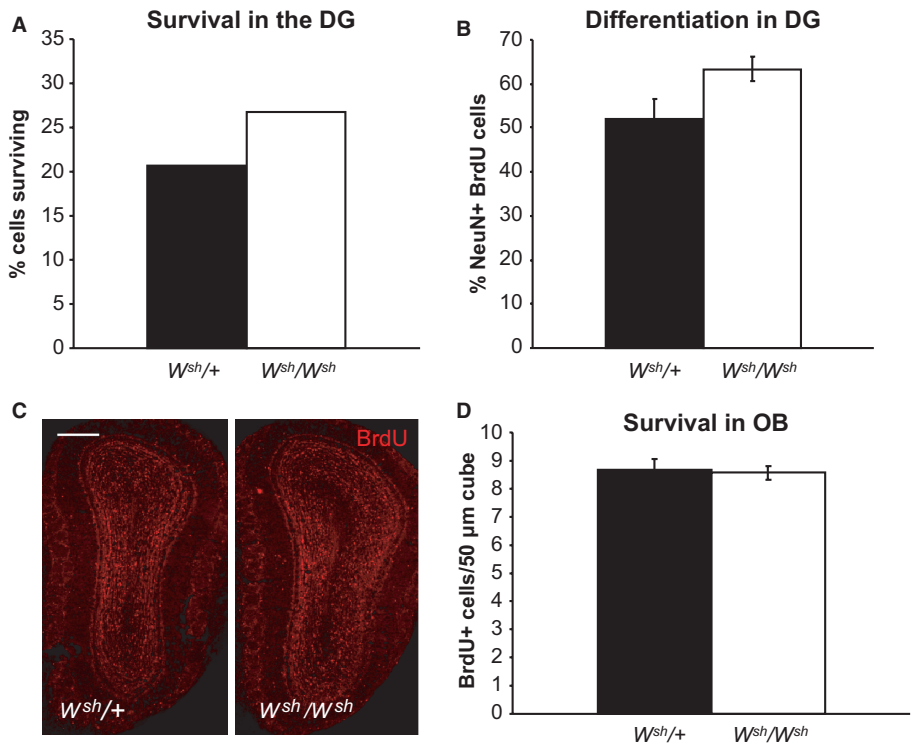

FIG. 7. Survival and differentiation of cells in dentate gyrus and olfactory bulb in $W^{sh}/+$ and W^{sh}/W^{sh} mice. (A) Histogram of the percentage BrdU+ cells surviving in the dentate gyrus for 28 days. (B) Percentage of surviving BrdU+ cells that were also NeuN+. (C) Representative photomicrographs of BrdU staining in the olfactory bulb of $W^{sh}/+$ and W^{sh}/W^{sh} mice. Scale bar = 300 μm. (D) Histogram of the number of BrdU+ cells in olfactory bulb.

TABLE 2. Plasma corticosterone levels in *Wsh/+* and littermate *Wsh/Wsh* mice

	$W^{sh}/+$ (X ± SEM)	W^{sh}/W^{sh} (X ± SEM)
Plasma corticosterone (ng/ml)	67.5 ± 16.6	66.2 ± 19.0

between W^{sh}/W^{sh} ($n = 7$) and $W^{sh}/+$ ($n = 7$) mice (Table 2; $t_{12} = 0.05$, $P > 0.05$).

Immunohistochemistry of c-kit receptor

The cellular localization of c-kit receptor in the WT mouse brain has previously been described (Zhang & Fedoroff, 1997). To examine c-kit receptor expression in the brain, we performed immunohistochemistry in hippocampus and cerebellum, and found no differences in the brain of W^{sh}/W^{sh} mice compared with $W^{sh}/+$ littermates (Fig. 8).

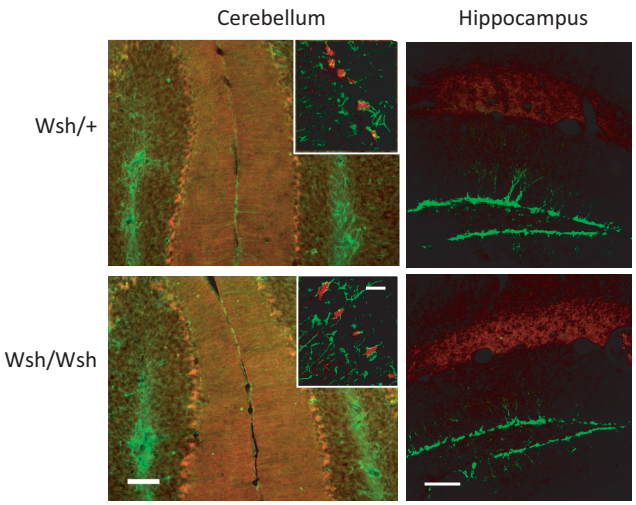

FIG. 8. c-kit receptor staining in $W^{sh}/+$ and W^{sh}/W^{sh} mice. c-kit receptor (red) staining is seen in the cerebellum (left) and hippocampus (right) in sections labeled with GFAP (green, cerebellum) or DCX (green, hippocampus). There were no differences detected between *Wsh/+* (top) and *Wsh/Wsh* (bottom) mice. Low-magnification scale bar = 100 μm, high-magnification inset scale bar = 20 μm.

SSRI administration

Given the known effects of SSRI treatment on serotonin signaling and neurogenesis in mice (Malberg *et al.*, 2000), we investigated whether fluoxetine treatment in W^{sh}/W^{sh} mice would reverse the deficit in neurogenesis (Fig. 9). W^{sh}/W^{sh} ($n = 17$) and $W^{sh}/+$ ($n = 16$) mice were assessed for cell proliferation by BrdU labeling following 35 days of treatment with fluoxetine or saline (Fig. 9A). The deficit in cell proliferation in W^{sh}/W^{sh} mice was replicated in these saline-treated animals. W^{sh}/W^{sh} mice had a ~40% reduction in the number of BrdU+ cells compared with $W^{sh}/+$ mice ($t_{13} = 4.05$, $P < 0.01$). Fluoxetine treatment resulted in an increase of BrdU+ cells, regardless of genotype ($F_{1,29} = 15.9$, $P < 0.01$). Fluoxetine increased the number of BrdU+ cells in the DG from 62.0 ± 4.4 to 90.2 ± 13.5 in $W^{sh}/+$ mice (Mann–Whitney, $P < 0.05$) and from 36.4 ± 4.5 to 107.8 ± 17.4 in W^{sh}/W^{sh} mice ($t_{15} = 3.76$, $P < 0.01$). This indicates that W^{sh}/W^{sh}

© 2012 The Authors. European Journal of Neuroscience © 2012 Federation of European Neuroscience Societies and Blackwell Publishing Ltd

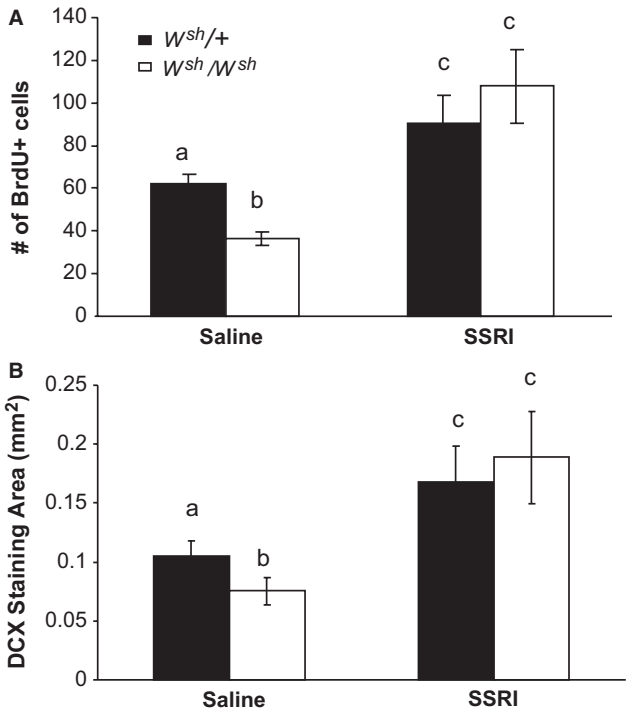

FIG. 9. SSRI treatment effects on neurogenesis in $W^{sh}/+$ and W^{sh}/W^{sh} mice. (A) The number of BrdU+ cells and (B) the area of DCX staining in response to saline and SSRI treatment. Different letters above the histogram bars indicate statistically significant differences at $P < 0.05$.

mice can sustain normal cell proliferation in the DG. There was no significant effect of genotype on the number of BrdU+ cells in fluoxetine-treated mice ($t_{16} = 0.80$, $P > 0.05$). There was a possible, but non-significant interaction of genotype and treatment ($F_{1,29} = 2.99$, $P = 0.09$). A similar reversal of the deficits in neurogenesis was also seen with the assessment of DCX immunoreactivity (Fig. 9B). Fluoxetine treatment increased DCX staining regardless of genotype ($F_{1,29} = 8.43$, $P < 0.01$) from 0.10 ± 0.01 to 0.18 ± 0.03 mm^2 in $W^{sh}/+$ mice and from 0.07 ± 0.01 to 0.19 ± 0.04 mm^2 in W^{sh}/W^{sh} mice ($t_{15} = 2.71$, $P < 0.05$). SSRI treatment increased DCX staining in W^{sh}/W^{sh} mice more than in $W^{sh}/+$ mice, resulting in no significant genotype effects following treatment ($t_{16} = 0.41$, $P > 0.05$).

Discussion

The present studies indicate that mast cells contribute to hippocampal physiology and function. We show that mast cells are a source of serotonin in the hippocampus. Mast cell-deficient W^{sh}/W^{sh} mice have deficits in hippocampus-dependent spatial learning and memory as assessed in the Morris water maze and radial arm maze. Additionally, mast cell-deficient W^{sh}/W^{sh} mice have reduced neurogenesis in hippocampus, but not in SVZ. Finally, elevating serotonin by treatment with the SSRI fluoxetine restores neurogenesis in the deficient animals.

Mast cells lie on the brain side of the blood–brain barrier, and are poised to act on adjacent neurons, glia and blood vessels (Silverman *et al.*, 2000). They are found in the brains of all mammals that have been studied (Olsson, 1969; Dropp, 1976, 1979; Persinger, 1979; Goldschmidt *et al.*, 1985; Gill & Rissman, 1998; Kriegsfeld *et al.*, 2003). Some fraction of central nervous system resident mast cells are always activated, releasing granules by piecemeal partial degranulation (Kraeuter Kops *et al.*, 1990; Dvorak *et al.*, 1992) even in animals at rest with no activation of other immune system components (Wilhelm *et al.*, 2000). The granular contents of mast cells can diffuse a great distance, and their granule remnants are seen up to 500 μm from the cell of origin (Ruoss *et al.*, 1991; Marszalek *et al.*, 1997; Nautiyal *et al.*, 2008). Their location in leptomeninges also enables release of mast cell mediators into the cerebrospinal fluid, allowing access to hippocampal parenchyma via diffusion (Proescholdt *et al.*, 2000). In summary, the data indicate that mast cells are present in the mouse brain throughout development and adulthood, that they contribute serotonin and possibly other mediators to nearby hippocampal tissue, and that they affect cell proliferation and behavior.

Altered serotonin signaling in the hippocampus is associated with reduced neurogenesis and deficits in spatial learning (Lucki, 1998; Gould, 1999; Benninghoff *et al.*, 2010). Additionally, mast cells are known to synthesize serotonin in both rodents (Ringvall *et al.*, 2008) and humans (Kushnir-Sukhov *et al.*, 2007) and to release serotonin following application of C48/80 (Lambracht-Hall *et al.*, 1990; Marathias *et al.*, 1991). Here we demonstrate mast cells can contribute serotonin to the caudal hippocampus (Fig. 3). Our data show that serotonin levels in the hippocampus of $W^{sh}/+$ but not W^{sh}/W^{sh} mice are elevated following stimulation of mast cells with C48/80. This serotonin is probably contributed both by mast cells within the hippocampus and by those lying in the nearby leptomeninges. As a control, we examined Tyr levels and found that these do not change following C48/80 stimulation. The lack of differences in resting serotonin levels between $W^{sh/+}$ and W^{sh}/W^{sh} may be due either to limits in assay sensitivity or to variability in mast cell numbers, rather than to the absence of differences between the groups. Overall, the results confirm a significant contribution of mast cells to the neuronal pool of serotonin in the hippocampus. That said, while the present studies focus on serotonin, it is possible that other mast cell mediators including histamine, nerve growth factor and cytokines also contribute to hippocampal physiology and hippocampus-dependent behavior.

The effects of SSRI administration suggest a deficit in serotonin signaling in the W^{sh}/W^{sh} mice. Administration of the SSRI fluoxetine does not correct the mutation in W^{sh}/W^{sh} mice, yet does increase hippocampal serotonin signaling (Malberg *et al.*, 2000) and augments cell proliferation by stimulating division of early progenitor cells (Encinas *et al.*, 2006). The levels of cell proliferation seen in W^{sh}/W^{sh} mice following chronic fluoxetine treatment are comparable with those of their $W^{sh}/+$ littermates (Fig. 8) and C57BL/6 WT mice in general (Santarelli *et al.*, 2003; Navailles *et al.*, 2008). Thus, the reduction in neurogenesis in W^{sh}/W^{sh} mice is not due to a defect in progenitor cells themselves or in their responses to serotonergic signaling. Following SSRI treatment, W^{sh}/W^{sh} mice show somewhat greater increases in cell proliferation than $W^{sh}/+$ mice, perhaps mediated by an increased sensitivity to the elevated serotonin levels. This may result from an increase in 5-HT1A or 5-HT2C receptor expression, as these subserve serotonin-mediated increases in neurogenesis (Benninghoff *et al.*, 2010). As previously reported for the C57BL/6 strain (Crowley *et al.*, 2005; Sugimoto *et al.*, 2008), we found no effect of SSRI treatment on depressive behaviors (data not shown).

Although we provide evidence in the SSRI studies that the observed hippocampal deficits in W^{sh}/W^{sh} mice may be accounted for by the mast cell deficit, the c-kit mutation may also contribute. Stem cell factor and c-kit receptor signaling in the hippocampus are implicated in spatial learning and memory and neurogenesis (Katafuchi *et al.*, 2000; Zhang & Sieber-Blum, 2009). However, c-kit receptor immunostaining in the brain reveals no difference between W^{sh}/W^{sh} and $W^{sh}/+$ mice (Fig. 8).

© 2012 The Authors. European Journal of Neuroscience © 2012 Federation of European Neuroscience Societies and Blackwell Publishing Ltd

Adult hippocampal neurogenesis is implicated in the regulation of emotionality and memory (Shors *et al.*, 2001; Snyder *et al.*, 2005; Sahay & Hen, 2007) and genetic ablation of neurogenesis throughout the brain produces major deficits in performance on spatial learning and memory tasks (Garthe *et al.*, 2009). This raises the possibility that the deficits in hippocampal neurogenesis may be causally related to deficits in spatial learning and memory in W^{sh}/W^{sh} mice. However, in the data presented here, the deficits of W^{sh}/W^{sh} mice on these tasks are more profound than previously reported following reduced neurogenesis. For example, following ablation of adult hippocampal neurogenesis, there is no effect on acquisition of hippocampal-dependent spatial learning and memory tasks such as the Morris water maze, radial arm maze and Y-maze (Snyder *et al.*, 2005; Saxe *et al.*, 2006, 2007; Clark *et al.*, 2008). In studies where deficits in performance are reported (Zhang *et al.*, 2008), they are much smaller than those seen here. These prior studies focused on the effects of reduced neurogenesis in adulthood. Possibly, the profound deficits in the W^{sh}/W^{sh} mouse deficits in spatial learning and memory (this study) and in emotionality behaviors (Nautiyal *et al.*, 2008) result from the absence of mast cell-dependent neurogenesis and decreased serotonin of mast cell origin during development. In support of this, decreased serotonin during development contributes to mood disorders such as anxiety and depression (reviewed by Daubert & Condron, 2010).

Overall these data highlight a striking instance of an immune system cell contribution to normal brain development and extend the existing body of work that shows that immune cells and their signaling molecules contribute to normal hippocampal function (Raison *et al.*, 2006; Ziv *et al.*, 2006; Goshen *et al.*, 2008; Koo & Duman, 2008). The consequences of inadequate immune activation during development may include an increased prevalence of hippocampus-related behavioral disorders, including anxiety and depression (reviewed by Rook & Lowry, 2008).

Acknowledgements

We thank Drs Matthew Butler, Michael Drew and Lance Kriegsfeld for their comments on earlier drafts of the manuscript, Dr Rene Hen for helpful discussions, and Dr Joseph LeSauter and Sharmin Ferdaus for technical assistance. Funding was provided by the following sources: F31 NIMH 084384 (to K.M.N.), NSF IOS 05-54514 (to R.S.), NSF DBI 320988 (to Barnard College), R21 NIMH 067782 (to R.S.), P30DA018310 (to J.V.S.) and R01 DE018866 (to J.V.S.); the content is solely the responsibility of the authors and does not necessarily represent the official views of the National Institutes of Health.

Abbreviations

BrdU, 5-bromo-2′-deoxyuridine; CE-LINF, capillary electrophoresis with laser induced native fluorescence; DCX, doublecortin; DG, dentate gyrus; GCL, granule cell layer; GFAP, glial fibrillary acidic protein; GFP, green fluorsecent protein; HBSS, Hank's balanced salt solution; NeuN, neuronal-specific nucleus protein; PN, postnatal day; SSRI, selective serotonin reuptake inhibitor; SVZ, subventricular zone; TB, toluidine blue; WT, wild-type.

References

Altman, H.J. & Normile, H.J. (1988) What is the nature of the role of the serotonergic nervous system in learning and memory: prospects for development of an effective treatment strategy for senile dementia. *Neurobiol. Aging*, **9**, 627–638.

Altman, H.J., Normile, H.J., Galloway, M.P., Ramirez, A. & Azmitia, E.C. (1990) Enhanced spatial discrimination learning in rats following 5,7-DHT-induced serotonergic deafferentation of the hippocampus. *Brain Res.*, **518**, 61–66.

Benninghoff, J., Gritti, A., Rizzi, M., Lamorte, G., Schloesser, R.J., Schmitt, A., Robel, S., Genius, J., Moessner, R., Riederer, P., Manji, H.K., Grunze, H., Rujescu, D., Moeller, H.J., Lesch, K.P. & Vescovi, A.L. (2010) Serotonin depletion hampers survival and proliferation in neurospheres derived from adult neural stem cells. *Neuropsychopharmacol.*, **35**, 893–903.

Bussolati, G. & Gugliotta, P. (1983) Nonspecific staining of mast cells by avidin-biotin-peroxidase complexes (ABC). *J. Histochem. Cytochem.*, **31**, 1419–1421.

Chen, C.C., Grimbaldeston, M.A., Tsai, M., Weissman, I.L. & Galli, S.J. (2005) Identification of mast cell progenitors in adult mice. *Proc. Natl. Acad. Sci. USA*, **102**, 11408–11413.

Clark, P.J., Brzezinska, W.J., Thomas, M.W., Ryzhenko, N.A., Toshkov, S.A. & Rhodes, J.S. (2008) Intact neurogenesis is required for benefits of exercise on spatial memory but not motor performance or contextual fear conditioning in C57BL/6J mice. *Neuroscience*, **155**, 1048–1058.

Crowley, J.J., Blendy, J.A. & Lucki, I. (2005) Strain-dependent antidepressant-like effects of citalopram in the mouse tail suspension test. *Psychopharmacology*, **183**, 257–264.

Daubert, E.A. & Condron, B.G. (2010) Serotonin: a regulator of neuronal morphology and circuitry. *Trends Neurosci.*, **33**, 424–434.

Dropp, J.J. (1976) Mast cells in mammalian brain. *Acta Anat. (Basel)*, **94**, 1–21.

Dropp, J.J. (1979) Mast cells in the human brain. *Acta Anat. (Basel)*, **105**, 505–513.

Duttlinger, R., Manova, K., Chu, T.Y., Gyssler, C., Zelenetz, A.D., Bachvarova, R.F. & Besmer, P. (1993) W-sash affects positive and negative elements controlling c-kit expression: ectopic c-kit expression at sites of kit-ligand expression affects melanogenesis. *Development*, **118**, 705–717.

Dvorak, A.M., McLeod, R.S., Onderdonk, A., Monahan-Earley, R.A., Cullen, J.B., Antonioli, D.A., Morgan, E., Blair, J.E., Estrella, P., Cisneros, R.L., Letourneau L., Morgan E., Silen W. & Cohen Z. (1992) Ultrastructural evidence for piecemeal and anaphylactic degranulation of human gut mucosal mast cells in vivo. *Int. Arch. Allergy Immunol.*, **99**, 74–83.

Encinas, J.M., Vaahtokari, A. & Enikolopov, G. (2006) Fluoxetine targets early progenitor cells in the adult brain. *Proc. Natl. Acad. Sci. USA*, **103**, 8233–8238.

Esposito, P., Gheorghe, D., Kandere, K., Pang, X., Connolly, R., Jacobson, S. & Theoharides, T.C. (2001) Acute stress increases permeability of the blood-brain-barrier through activation of brain mast cells. *Brain Res.*, **888**, 117–127.

Florenzano, F. & Bentivoglio, M. (2000) Degranulation, density, and distribution of mast cells in the rat thalamus: a light and electron microscopic study in basal conditions and after intracerebroventricular administration of nerve growth factor. *J. Comp. Neurol.*, **424**, 651–669.

Fuller, R.R., Moroz, L.L., Gillette, R. & Sweedler, J.V. (1998) Single neuron analysis by capillary electrophoresis with fluorescence spectroscopy. *Neuron*, **20**, 173–181.

Galli, S.J., Grimbaldeston, M. & Tsai, M. (2008) Immunomodulatory mast cells: negative, as well as positive, regulators of immunity. *Nat. Rev. Immunol.*, **8**, 478–486.

Garthe, A., Behr, J. & Kempermann, G. (2009) Adult-generated hippocampal neurons allow the flexible use of spatially precise learning strategies. *PLoS ONE*, **4**, e5464.

Gaspar, P., Cases, O. & Maroteaux, L. (2003) The developmental role of serotonin: news from mouse molecular genetics. *Nat. Rev. Neurosci.*, **4**, 1002–1012.

Gill, C.J. & Rissman, E.F. (1998) Mast cells in the neonate musk shrew brain: implications for neuroendocrine immune interactions. *Brain Res. Dev. Brain Res.*, **111**, 129–136.

Goldschmidt, R.C., Hough, L.B. & Glick, S.D. (1985) Rat brain mast cells: contribution to brain histamine levels. *J. Neurochem.*, **44**, 1943–1947.

Goshen, I., Kreisel, T., Ben-Menachem-Zidon, O., Licht, T., Weidenfeld, J., Ben-Hur, T. & Yirmiya, R. (2008) Brain interleukin-1 mediates chronic stress-induced depression in mice via adrenocortical activation and hippocampal neurogenesis suppression. *Mol. Psychiatry*, **13**, 717–728.

Gould, E. (1999) Serotonin and hippocampal neurogenesis. *Neuropsychopharmacol.*, **21**, 46S–51S.

Gould, E., Woolley, C.S. & McEwen, B.S. (1991) Adrenal steroids regulate postnatal development of the rat dentate gyrus: I. Effects of glucocorticoids on cell death. *J. Comp. Neurol.*, **313**, 479–485.

Gray, J.A. & McNaughton, N. (1983) Comparison between the behavioural effects of septal and hippocampal lesions: a review. *Neurosci. Biobehav. Rev.*, **7**, 119–188.

Grimbaldeston, M.A., Chen, C.C., Piliponsky, A.M., Tsai, M., Tam, S.Y. & Galli, S.J. (2005) Mast cell-deficient W-sash c-kit mutant Kit W-sh/W-sh mice as a model for investigating mast cell biology in vivo. *Am. J. Pathol.*, **167**, 835–848.

Gundersen, H.J. & Jensen, E.B. (1987) The efficiency of systematic sampling in stereology and its prediction. *J. Microsc.*, **147**, 229–263.

© 2012 The Authors. European Journal of Neuroscience © 2012 Federation of European Neuroscience Societies and Blackwell Publishing Ltd

Hatcher, N.G., Atkins, N. Jr, Annangudi, S.P., Forbes, A.J., Kelleher, N.L., Gillette, M.U. & Sweedler, J.V. (2008) Mass spectrometry-based discovery of circadian peptides. *Proc. Natl. Acad. Sci. USA*, **105**, 12527–12532.

Hendrix, S., Warnke, K., Siebenhaar, F., Peters, E.M., Nitsch, R. & Maurer, M. (2006) The majority of brain mast cells in B10.PL mice is present in the hippocampal formation. *Neurosci. Lett.*, **392**, 174–177.

Hodges, H. (1996) Maze procedures: the radial-arm and water maze compared. *Brain Res. Cogn. Brain Res.*, **3**, 167–181.

Katafuchi, T., Li, A.J., Hirota, S., Kitamura, Y. & Hori, T. (2000) Impairment of spatial learning and hippocampal synaptic potentiation in c-kit mutant rats. *Learn. Mem.*, **7**, 383–392.

Kitamura, Y. & Fujita, J. (1989) Regulation of mast cell differentiation. *BioEssays*, **10**, 193–196.

Koo, J.W. & Duman, R.S. (2008) IL-1beta is an essential mediator of the antineurogenic and anhedonic effects of stress. *Proc. Natl. Acad. Sci. USA*, **105**, 751–756.

Kovács, K.J. & Larson, A.A. (2006) Mast cells accumulate in the anogenital region of somatosensory thalamic nuclei during estrus in female mice. *Brain Res.*, **1114**, 85–97.

Kraeuter Kops, S., Theoharides, T.C., Cronin, C.T., Kashgarian, M.G. & Askenase, P.W. (1990) Ultrastructural characteristics of rat peritoneal mast cells undergoing differential release of serotonin without histamine and without degranulation. *Cell Tissue Res.*, **262**, 415–424.

Kriegsfeld, L.J., Hotchkiss, A.K., Demas, G.E., Silverman, A.J., Silver, R. & Nelson, R.J. (2003) Brain mast cells are influenced by chemosensory cues associated with estrus induction in female prairie voles (*Microtus ochrogaster*). *Horm. Behav.*, **44**, 377–384.

Kruskal, W.H. & Wallis, W.A. (1952) Use of ranks in one-criterion variance analysis. *J. Am. Stat. Assoc.*, **47**, 583–621.

Kushnir-Sukhov, N.M., Brown, J.M., Wu, Y., Kirshenbaum, A. & Metcalfe, D.D. (2007) Human mast cells are capable of serotonin synthesis and release. *J. Allergy Clin. Immunol.*, **119**, 498–499.

Lambracht-Hall, M., Konstantinidou, A.D. & Theoharides, T.C. (1990) Serotonin release from rat brain mast cells *in vitro*. *Neuroscience*, **39**, 199–207.

Lauder, J.M. (1990) Ontogeny of the serotonergic system in the rat: serotonin as a developmental signal. *Ann. NY Acad. Sci.*, **600**, 297–313; discussion 314.

Lauder, J.M. & Krebs, H. (1978) Serotonin as a differentiation signal in early neurogenesis. *Dev. Neurosci.*, **1**, 15–30.

Lucki, I. (1998) The spectrum of behaviors influenced by serotonin. *Biol. Psychiatry*, **44**, 151–162.

Malberg, J.E., Eisch, A.J., Nestler, E.J. & Duman, R.S. (2000) Chronic antidepressant treatment increases neurogenesis in adult rat hippocampus. *J. Neurosci.*, **20**, 9104–9110.

Marathias, K., Lambracht-Hall, M., Savala, J. & Theoharides, T.C. (1991) Endogenous regulation of rat brain mast cell serotonin release. *Int. Arch. Allergy Appl. Immunol.*, **95**, 332–340.

Marshall, J.S. (2004) Mast-cell responses to pathogens. *Nat. Rev. Immunol.*, **4**, 787–799.

Marszalek, P.E., Farrell, B., Verdugo, P. & Fernandez, J.M. (1997) Kinetics of release of serotonin from isolated secretory granules. II. Ion exchange determines the diffusivity of serotonin. *Biophys. J.*, **73**, 1169–1183.

Mazer, C., Muneyyirci, J., Taheny, K., Raio, N., Borella, A. & Whitaker-Azmitia, P. (1997) Serotonin depletion during synaptogenesis leads to decreased synaptic density and learning deficits in the adult rat: a possible model of neurodevelopmental disorders with cognitive deficits. *Brain Res.*, **760**, 68–73.

Menétrey, D. & Dubayle, D.A. (2003) A one-step dual-labeling method for antigen detection in mast cells. *Histochem. Cell Biol.*, **120**, 435–442.

Meshi, D., Drew, M.R., Saxe, M., Ansorge, M.S., David, D., Santarelli, L., Malapani, C., Moore, H. & Hen, R. (2006) Hippocampal neurogenesis is not required for behavioral effects of environmental enrichment. *Nat. Neurosci.*, **9**, 729–731.

Morris, R. (1984) Developments of a water-maze procedure for studying spatial learning in the rat. *J. Neurosci. Methods*, **11**, 47–60.

Nautiyal, K.M., Ribeiro, A.C., Pfaff, D.W. & Silver, R. (2008) Brain mast cells link the immune system to anxiety-like behavior. *Proc. Natl. Acad. Sci. USA*, **105**, 18053–18057.

Nautiyal, K.M., Liu, C., Dong, X. & Silver, R. (2011) Blood-borne donor mast cell precursors migrate to mast cell-rich brain regions in the adult mouse. *J. Neuroimmunol.*, **240**, 142–146.

Navailles, S., Hof, P.R. & Schmauss, C. (2008) Antidepressant drug-induced stimulation of mouse hippocampal neurogenesis is age-dependent and altered by early life stress. *J. Comp. Neurol.*, **509**, 372–381.

Olsson, Y. (1969) Mast cells in the nervous system. *Int. Rev. Cytol.*, **24**, 27–70.

Otsu, N. (1979) A threshold selection method from grey-level histograms. *IEEE Trans. Sys. Man. Cyber.*, **9**, 62–66.

Paxinos, G. & Franklin, K.B.J. (2004) *The Mouse Brain in Sterotaxic Coordinates*. Academic Press, San Diego, CA.

Persinger, M.A. (1979) Brain mast cell numbers in the albino rat: sources variability. *Behav. Neural. Biol.*, **25**, 380–386.

Presnell, J.K. & Schreibman, M.P. (1997) *Humason's Animal Tissue Techniques*, 5th edn. The Johns Hopkins University Press, Baltimore, MD.

Proescholdt, M.G., Hutto, B., Brady, L.S. & Herkenham, M. (2000) Studies of cerebrospinal fluid flow and penetration into brain following lateral ventricle and cisterna magna injections of the tracer [^{14}C]inulin in rat. *Neuroscience*, **95**, 577–592.

Raison, C.L., Capuron, L. & Miller, A.H. (2006) Cytokines sing the blues: inflammation and the pathogenesis of depression. *Trends Immunol.*, **27**, 24–31.

Ringvall, M., Ronnberg, E., Wernersson, S., Duelli, A., Henningsson, F., Abrink, M., Garcia-Faroldi, G., Fajardo, I. & Pejler, G. (2008) Serotonin and histamine storage in mast cell secretory granules is dependent on serglycin proteoglycan. *J. Allergy Clin. Immunol.*, **121**, 1020–1026.

Rook, G.A. & Lowry, C.A. (2008) The hygiene hypothesis and psychiatric disorders. *Trends Immunol.*, **29**, 150–158.

Ruoss, S.J., Gold, W.M. & Caughey, G.H. (1991) Mast cell exocytosis: evidence that granule proteoglycan processing is not coupled to degranulation. *Biochem. Biophys. Res. Commun.*, **179**, 140–146.

Sahay, A. & Hen, R. (2007) Adult hippocampal neurogenesis in depression. *Nat. Neurosci.*, **10**, 1110–1115.

Santarelli, L., Saxe, M., Gross, C., Surget, A., Battaglia, F., Dulawa, S., Weisstaub, N., Lee, J., Duman, R., Arancio, O., Belzung, C. & Hen, R. (2003) Requirement of hippocampal neurogenesis for the behavioral effects of antidepressants. *Science*, **301**, 805–809.

Saxe, M.D., Battaglia, F., Wang, J.W., Malleret, G., David, D.J., Monckton, J.E., Garcia, A.D., Sofroniew, M.V., Kandel, E.R., Santarelli, L., Hen, R. & Drew, M.R. (2006) Ablation of hippocampal neurogenesis impairs contextual fear conditioning and synaptic plasticity in the dentate gyrus. *Proc. Natl. Acad. Sci. USA*, **103**, 17501–17506.

Saxe, M.D., Malleret, G., Vronskaya, S., Mendez, I., Garcia, A.D., Sofroniew, M.V., Kandel, E.R. & Hen, R. (2007) Paradoxical influence of hippocampal neurogenesis on working memory. *Proc. Natl. Acad. Sci. USA*, **104**, 4642–4646.

Scoville, W.B. & Milner, B. (1957) Loss of recent memory after bilateral hippocampal lesions. *J. Neurol. Neurosurg. Psychiatry*, **20**, 11–21.

Shors, T.J., Miesegaes, G., Beylin, A., Zhao, M., Rydel, T. & Gould, E. (2001) Neurogenesis in the adult is involved in the formation of trace memories. *Nature*, **410**, 372–376.

Silverman, A.J., Millar, R.P., King, J.A., Zhuang, X. & Silver, R. (1994) Mast cells with gonadotropin-releasing hormone-like immunoreactivity in the brain of doves. *Proc. Natl. Acad. Sci. USA*, **91**, 3695–3699.

Silverman, A.J., Sutherland, A.K., Wilhelm, M. & Silver, R. (2000) Mast cells migrate from blood to brain. *J. Neurosci.*, **20**, 401–408.

Snyder, J.S., Hong, N.S., McDonald, R.J. & Wojtowicz, J.M. (2005) A role for adult neurogenesis in spatial long-term memory. *Neuroscience*, **130**, 843–852.

Squires, L.N., Talbot, K.N., Rubakhin, S.S. & Sweedler, J.V. (2007) Serotonin catabolism in the central and enteric nervous systems of rats upon induction of serotonin syndrome. *J. Neurochem.*, **103**, 174–180.

Sugimoto, Y., Kajiwara, Y., Hirano, K., Yamada, S., Tagawa, N., Kobayashi, Y., Hotta, Y. & Yamada, J. (2008) Mouse strain differences in immobility and sensitivity to fluvoxamine and desipramine in the forced swimming test: analysis of serotonin and noradrenaline transporter binding. *Eur. J. Pharmacol.*, **592**, 116–122.

Tharp, M.D., Seelig, L.L. Jr, Tigelaar, R.E. & Bergstresser, P.R. (1985) Conjugated avidin binds to mast cell granules. *J. Histochem. Cytochem.*, **33**, 27–32.

Watanabe, Y., Gould, E., Daniels, D.C., Cameron, H. & McEwen, B.S. (1992) Tianeptine attenuates stress-induced morphological changes in the hippocampus. *Eur. J. Pharmacol.*, **222**, 157–162.

Wilhelm, M., King, B., Silverman, A.J. & Silver, R. (2000) Gonadal steroids regulate the number and activational state of mast cells in the medial habenula. *Endocrinology*, **141**, 1178–1186.

Yan, W., Wilson, C.C. & Haring, J.H. (1997) Effects of neonatal serotonin depletion on the development of rat dentate granule cells. *Brain Res. Dev. Brain Res.*, **98**, 177–184.

© 2012 The Authors. European Journal of Neuroscience © 2012 Federation of European Neuroscience Societies and Blackwell Publishing Ltd

Yang, M., Chien, C. & Lu, K. (1999) Morphological, immunohistochemical and quantitative studies of murine brain mast cells after mating. *Brain Res.*, **846**, 30–39.

Yirmiya, R. & Goshen, I. (2011) Immune modulation of learning, memory, neural plasticity and neurogenesis. *Brain Behav. Immun.*, **25**, 181–213.

Zhang, S.C. & Fedoroff, S. (1997) Cellular localization of stem cell factor and c-kit receptor in the mouse nervous system. *J. Neurosci. Res.*, **47**, 1–15.

Zhang, Z.J. & Sieber-Blum, M. (2009) Essential role of stem cell factor signaling in primary sensory neuron development. *Dev. Neurosci.*, **31**, 202–211.

Zhang, C.L., Zou, Y., He, W., Gage, F.H. & Evans, R.M. (2008) A role for adult TLX-positive neural stem cells in learning and behaviour. *Nature*, **451**, 1004–1007.

Zhou, F.C. & Azmitia, E.C. (1983) Effects of 5,7-dihydroxytryptamine on HRP retrograde transport from hippocampus to midbrain raphe nuclei in the rat. *Brain Res. Bull.*, **10**, 445–451.

Zhuang, X., Silverman, A.J. & Silver, R. (1993) Reproductive behavior, endocrine state, and the distribution of GnRH-like immunoreactive mast cells in dove brain. *Horm. Behav.*, **27**, 283–295.

Zhuang, X., Silverman, A.J. & Silver, R. (1999) Distribution and local differentiation of mast cells in the parenchyma of the forebrain. *J. Comp. Neurol.*, **408**, 477–488.

Ziv, Y., Ron, N., Butovsky, O., Landa, G., Sudai, E., Greenberg, N., Cohen, H., Kipnis, J. & Schwartz, M. (2006) Immune cells contribute to the maintenance of neurogenesis and spatial learning abilities in adulthood. *Nat. Neurosci.*, **9**, 268–275.

© 2012 The Authors. European Journal of Neuroscience © 2012 Federation of European Neuroscience Societies and Blackwell Publishing Ltd